The Free Internet Journal for Organic Chemistry

Paper

Archive for Organic Chemistry

Arkivoc **2020**, part vi, 139-154

Synthesis of novel bisphosphorylimides based on Staudinger reaction

Lais Weber[a], Michael Weinert[b], Daniela Goedderz[a], Olaf Fuhr[c], and Manfred Döring[a]

[a]*Fraunhofer Institute for Structural Durability and System Reliability LBF, 64289 Darmstadt, Germany*
[b]*Fraunhofer Institute for Chemical Technology ICT, 76327 Pfinztal, Germany*
[c]*Institute of Nanotechnology (INT) and Karlsruhe Nano Micro Facility (KNMF), Karlsruhe Institute of Technology, 76344 Eggenstein-Leopoldshafen, Germany*
Email: manfred.doering@lbf.fraunhofer.de

Received 01-08-2020 **Accepted** 04-23-2020 **Published on line** 05-04-2020

Abstract

A series of bisphosphorylimides based on the reaction sequence of Atherton-Todd and Staudinger reaction were synthesized. These bisphosphorylimides containing phosphorus in different chemical environments, while the reaction sequence is using mild conditions and moreover can be synthesized in an one-pot procedure. The molecular structures were revealed by nuclear magnetic resonance spectroscopy and x-ray crystallography. The stability of the bisphosphorylimides against hydrolysis and thermal influences was tested which allows an initial estimation about the usage as flame retardant.

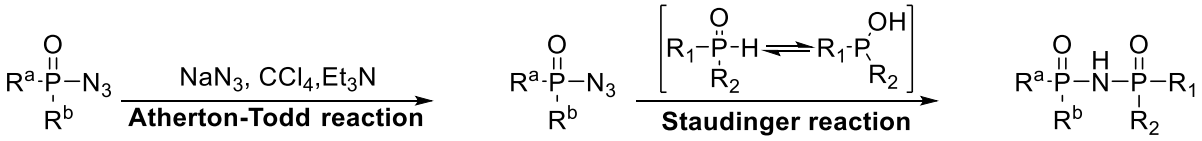

Keywords: 9,10-Dihydro-9-oxa-10-phosphaphenanthrene-10-oxide, phosphorus, bisphosphorylimides, Staudinger reaction, Atherton-Todd reaction

Introduction

Bisphosphorylimides are organophosphorus compounds with a general structural unit $R_2P(O)$-NH-$(O)PR_2$. Due to the biological activity phosphorus-nitrogen compounds are used as catalysts[1] while playing a decisive role as a ligand.[2-6]

In recent years, the usage as phosphorus-nitrogen based flame retardants gets more attention and due to its versatility and effectiveness, phosphorus is a promising element to replace the widespread halogenated flame retardants.[7-11] Phosphorus based flame retardants have shown direct correlation between the point of attack during burning and the chemical structure surrounding the phosphorus species. The combination of phosphorus groups with different chemical environments within one compound is a promising approach for an efficient flame retardant mechanism in gas and condensed phase, especially for composite materials due to the need of efficiency in both phases.[12-16]

From a synthetic point of view, the Staudinger reaction could achieve a facile and fast routine to access nitrogen-containing compounds with phosphorus in different environments to enable the previous mentioned efficient mode of action in gas and condensed phase.[17-23]

Various azides including carbonyl, sulfonyl and phosphoryl azides have been employed in this reaction.[18,20,24] These azides can be easily obtained from the corresponding chlorinated species. Also, Shi et al. described the direct azidation of phosphites under modified Atherton-Todd conditions in which the chlorides occur as intermediates.[25] Riesel et al. combined the Atherton-Todd and the Staudinger reaction in a one-pot synthesis.[21]

Aside from phosphazenes the corresponding structural element P-N-P however is described less frequently in literature and synthesis of nitrogen bridged di-phosphorus compounds often contain either extensive procedures, bad atom efficiency or hazardous byproducts.[26-29]

We successfully show the accessibility of apparent pentavalent phosphorus compounds via Staudinger reaction, taking advantage of the prototropic tautomeric equilibrium of phosphinylidene to synthesize several new flame retardants with phosphorus in different environments.

Results and Discussion

The intended DOPO-based bisphosphorylimides were prepared as shown in Scheme 1A. DOPO-N_3 was obtained of either by azidation of DOPO under Atherton-Todd conditions in 92% yield or by a metathesis reaction DOPO-Cl with NaN_3 in 90% yield as yellow oil. Column chromatography with EE/hexane (60:40) on silica gel yielded the spectroscopically pure product as a colorless oil (R_f = 0.66). For consecutive reactions, filtration of the crude product over silica gel and further extraction with $NaHCO_3/H_2O$ was sufficient.

Diphenyl phosphoryl azide (DPPA) based bisphosphorylimides were prepared by a one-step procedure starting with the azide followed directly by Staudinger reaction (Scheme 1B).

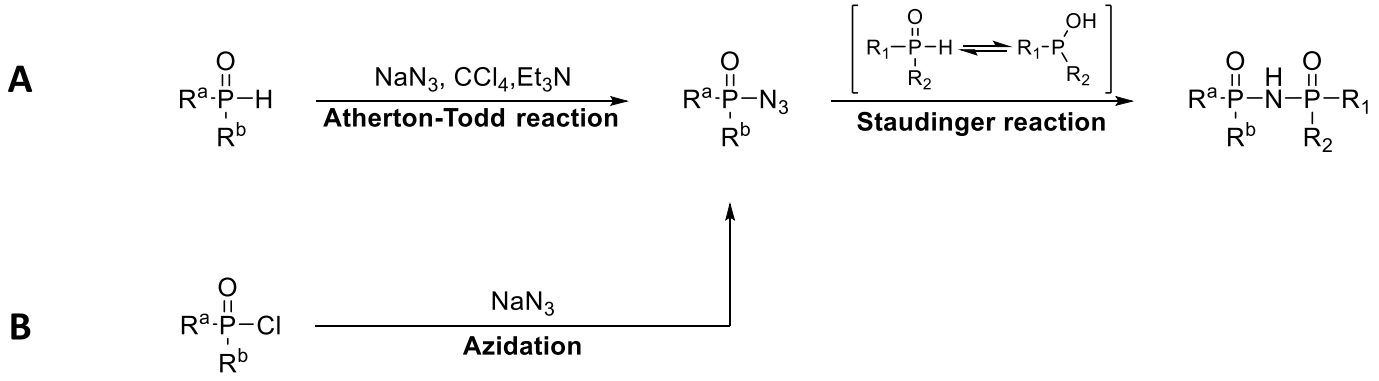

Scheme 1. General synthetic strategy of bisphosphorylimides via Atherton-Todd or direct Azidation followed by Staudinger reaction.

Compared to the Staudinger reaction procedure from trivalent phosphorus species (phosphanes and phosphites) the conversion of the apparent pentavalent species (diarylphosphine oxid, diarylphosphinate, dialkyl- and diarylphosphonate) needs more time and higher reaction temperatures. The complete conversion was achieved after five hours of reaction time at 80°C in acetonitrile. Scheme 2 is showing the synthesized DPPA- and DOPO-N_3-based products.

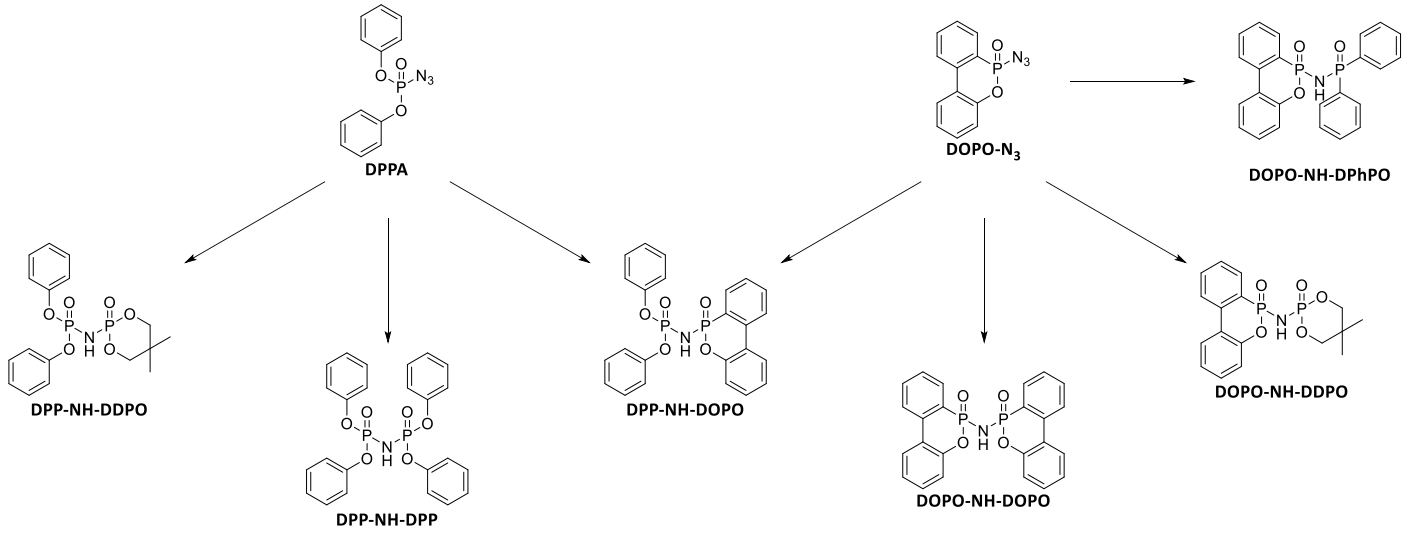

Scheme 2. Synthesis of DPPA- and DOPO-based bisphosphorylimides via Staudinger reaction.

For synthetic comparison and comparative analysis, the known reaction sequences from literature were studied and two examples are mentioned below. Nielsen has prepared bisphosphorylimides via condensation reaction from phosphorus chlorides and amines with sodium hydride.[27] Wilkening et al. has researched peptide conjugation via Staudinger reaction, while preparing the trivalent phosphorus species using trimethylsilyl protecting groups.[29]

Also the conversion of sulfonyl azides was studied as shown in Scheme 3, starting with p-toluenesulfonyl chloride (p-TSS-Cl) followed by azidation with NaN_3 and Staudinger reaction similar to the previous described procedure of DPPA to form the desired imide salt.

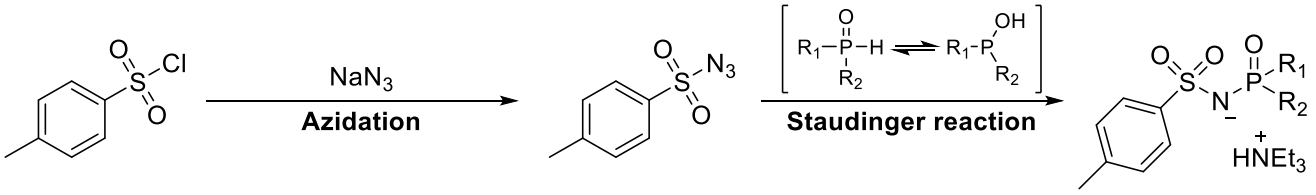

Scheme 3. Synthesis of p-toluenesulfonyl chloride-based bisphosphorylimides (pTSS-NH-DOPO) via Staudinger reaction.

The azidation without utilizing the Atherton-Todd reaction followed by Staudinger reaction was performed successively in a one-pot synthesis procedure, without any purification between the reaction steps. The conversion during the different procedures was confirmed using ^{31}P and ^{1}H-NMR. ^{1}H-NMR spectra can show the characteristic signal pattern of DOPO or p-toluolsulfonyl species. ^{31}P-NMR spectra indicate the $^{2}J_{PP}$ coupling besides DPP-NH-DPP, which shows a singlet due to coincidence.

Crystal structure analysis. The bisphosphorylimides DOPO-NH-DOPO and DOPO-NH-DPhPO where recrystallized from isopropyl alcohol, whereas DPP-NH-DPP and DPP-NH-DOPO were recrystallized from chloroform to get single crystals useful for x-ray diffraction analysis. Selected bonds and angles are summarized in Table 1. These data were discussed and compared among one another and additionally with a comparable crystalline structure from literature (Figure 1). Crystallographic data and structure refinement details are shown in the supplementary information.

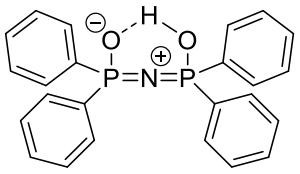

Figure 1. Comparable crystalline structure DPhPO-NH-DPhPO.[30]

Table 1. Summary of selected bond lengths in Å and bond angles in ° from synthesized products and selected reference compounds

Compounds	Bond lengths (Å)					Bond angles (°)
	P1-N1	P2-N1	P1=O	P2=O	N1---O4/3	P-N-P
DOPO-NH-DOPO	1.646(0)	1.658(8)	1.457(1)	1.473(1)	2.795(7)	130.5(8)
DOPO-NH-DPhPO	1.640(9)	1.665(0)	1.479(1)	1.464(4)	2.724(0)	130.1(8)
DPP-NH-DPP	1.633(3)	1.653(8)	1.463(8)	1.447(1)	2.740(7)	130.0(1)
DPP-NH-DOPO	1.649(5)	1.637(0)	1.470(7)	1.459(9)	2.731(7)	132.5(4)
DPhPO-NH-DPhPO[30]	1.535(1)	1.535(1)	1.519(2)	1.519(2)	-	180

Staudinger reaction using the prototropic tautomeric equilibrium of phosphinylidene could lead to two different tautomeric products (Figure 2). To verify either structure, single-crystal X-ray analysis was used. The

location of the hydrogen atom can be certainly identified at the nitrogen position, as seen in the crystal structure (Figure 3). Thereby the imide structure, rather than the phosphorylated iminophosphorane structure, can be verified for the synthesized di-phosphorus compounds.

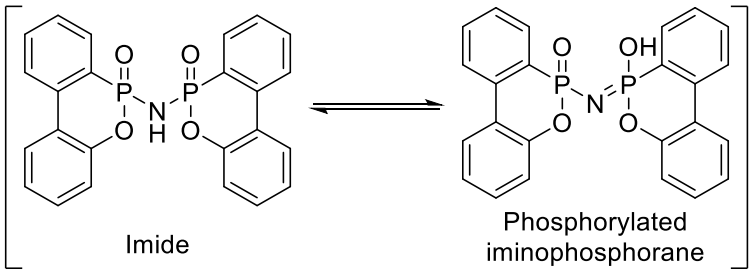

Figure 2. Possible structures resulting from DOPO-based Staudinger reaction.

The torsion angles of both ring elements in one DOPO-NH-DOPO are distinct from each other (P1 19.03° and P2 11.59°), therefore the structure does not contain a symmetric element. Remarkably is the syn conformation of both oxygen atoms O2 and O4, which is caused by the intramolecular π-π-interaction. Both ring systems of the DOPO-NH-DOPO (Figure2) structure are aligned almost parallel (Angle 12.29°) with a distance of (3.64 ± 0.29) Å between the rings.

The crystallographic data also show the existence of dimers of the above-mentioned single crystal structure of DOPO-NH-DOPO. Here, the oxygen atom O4 of each DOPO-NH-DOPO participates in an intermolecular hydrogen bond, while the oxygen atoms O2 remain free. Therefore, the lengths and angles of the bonds to O2 and O4 differ. The bond length P1-O2 with 1.4571 Å is shorter than the length P2-O4, which is 1.4731 Å.

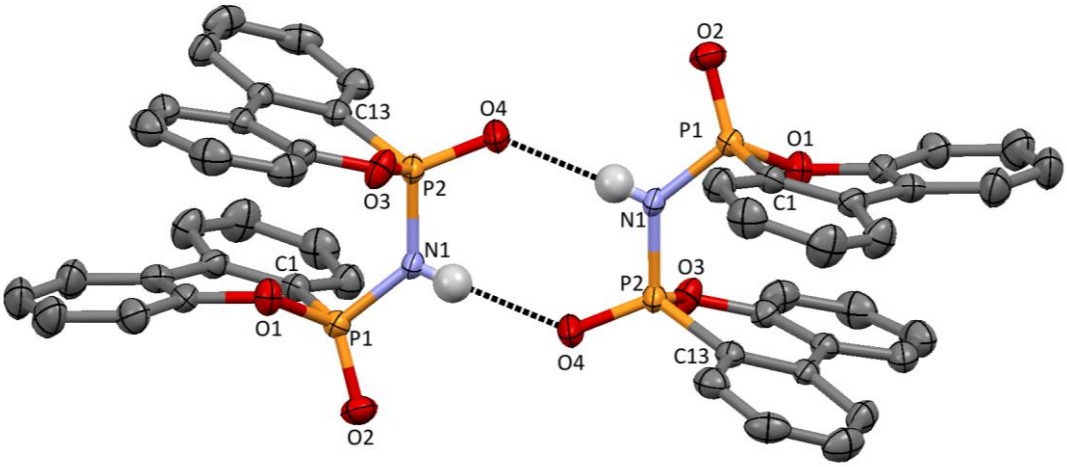

Figure 3. Dimeric molecular structure of DOPO-NH-DOPO. For clarity, H-atoms of aromatic rings are omitted.

Besides DOPO-NH-DOPO, also DPP-NH-DOPO (Figure 4) shows the syn conformation of both oxygen atoms O2 and O5. The oxygen atom O2 participates in the intermolecular hydrogen bond, whereas the oxygen O5 does not. The bond length P2-O5 with 1.4599 Å is smaller than P1-O2 with 1.4707 Å.

In the crystal structure of DPP-NH-DOPO an almost parallel alignment (Angle 6.51°) of one aromatic ring (C13-C18) with another aromatic ring of the DOPO unit with a distance of (3.16 ± 0.21) Å can be observed. The distance between the interacting π-systems of both structures is in the expected range of shifted π-systems as

benzene or nitrogen containing aromatic cycles (3.3-3.8 Å), in which the second compound ranges on the bottom of the scale.[31,32]

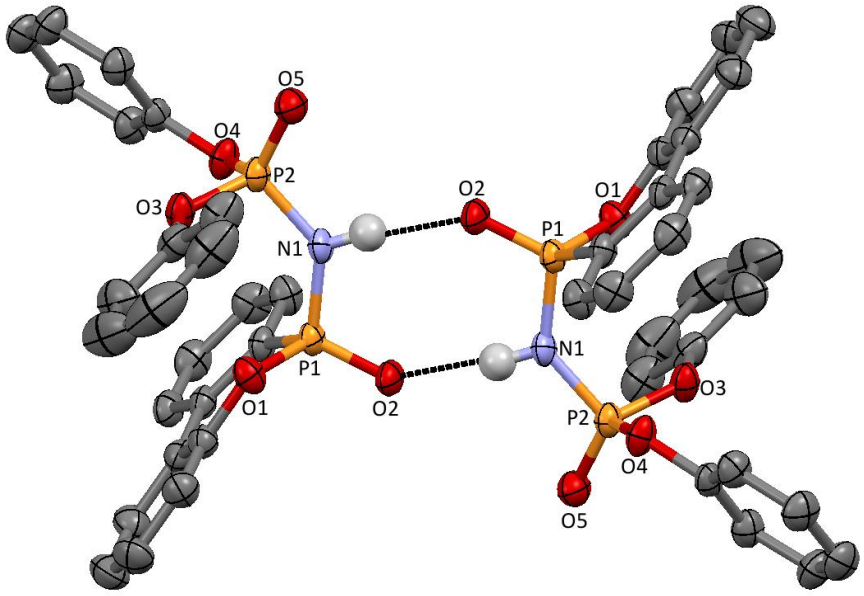

Figure 4. Dimeric molecular structure of DPP-NH-DOPO. For clarity, H-atoms of aromatic rings are omitted.

On the contrary, DOPO-DOPS-anhydride shows syn-conformation but no parallel alignment of the DOPO-units. In this case, sulfur acts as disruptive element and interferes with the orientation. The angle between the planes is 55.63°.[33] According to literature this syn-conformation could be observed before containing larger bridges between the interacting DOPO-units and can be verified for example for urea and hydroquinone bridged compounds.[34,35] Urea-bridged DOPO is showing syn-conformation with an similar angle (39.82°) as DOPO-DOPS-anhydride and has a significant larger distance between the planes of 7.26 ± 0.84 Å as the new bisphosphorylimides. Hydroquinone-bridged DOPO structures display an angle of 10.98° and a distance of 3.41 ± 0.22 Å and is with these values closer to bisphosphorylimides.

Usually the majority of structurally related compounds of the type $(RO)_2P(X)$-NH-$P(Y)(OR')_2$ with X, Y = O, S and R, R' = Ph, 2-Me–Ph, 3-Me–Ph, 4-Me–Ph, as well as $Ph_2P(S)$-NH-$P(S)Ph_2$ are present in an anti-conformation.[28] These anti conformations can be verified in the synthesized structures DPP-NH-DPP and DOPO-NH-DPhPO. In these structures, no intramolecular π-stacking was observed.

These structures also exist as a dimer connected with hydrogen bonds. The hydrogen located on the nitrogen and oxygen facing the same direction are participating in two hydrogen bonds and form the dimer. The lengths of the phosphorus and oxygen bonds in DPP-NH-DPP differ from 1.4638 Å (P1-O3) within the hydrogen bond to 1.4471 Å (P2-O6) between the not participating oxygen. Analog in the DOPO-NH-DPhPO structure, we can see the same difference in bond lengths. P1-O2 participates in the hydrogen bond with a length of 1.4791 Å and is therefore longer than the corresponding P2-O3 bond with 1.4644 Å, which is not participating.

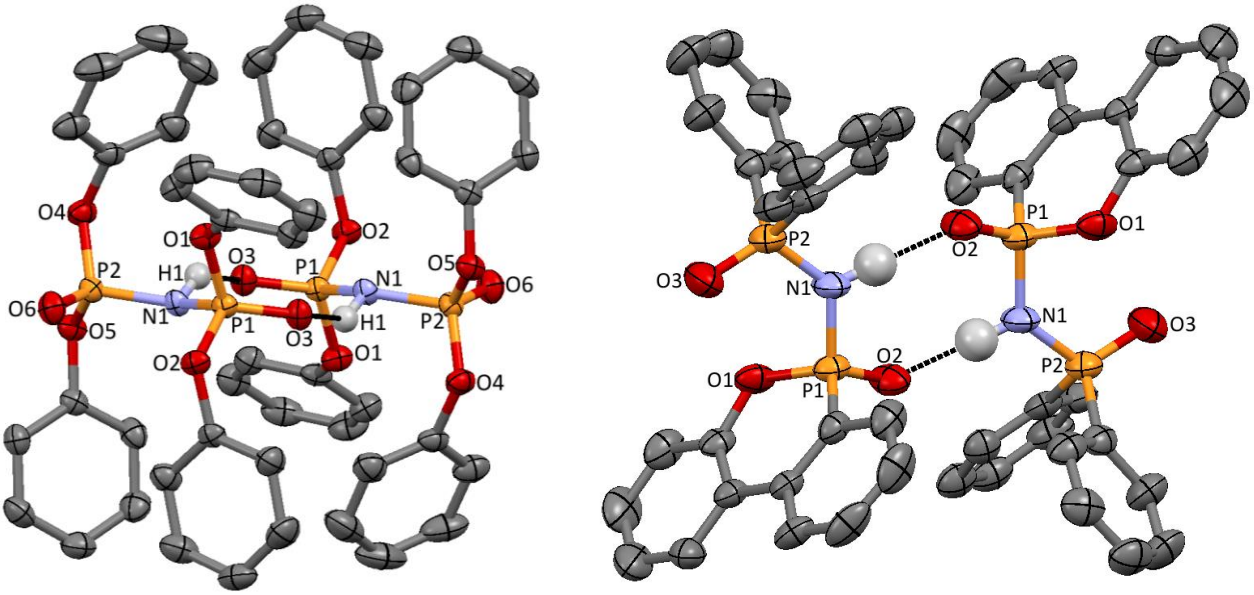

Figure 5. Dimeric structure of DPP-NH-DPP (left) and DOPO-NH-DPhPO (right).

These dimeric existences and different bond lengths are analogue to the characteristic crystal structures already described in literature.[30,36]

Regarding the bond lengths of the synthesized compounds and the structural data found in literature, a disparity can be observed. While the P-N-bond length in the new synthesized bisphosphorylimides are ranging around 1.648 Å, which is considered single-bond length, and are not showing much variation among the new molecules, the reference structure contains a bond with a length of 1.535 Å, which is regarded as a length of double-bonds. This difference in structure also applies to the P-N-P angles.[37]

Comparing the P-N-P angles of all the synthesized products are showing only small variations. The angles range around 130° with a variation that does not exceed 1°. The angle of 130° is distinct from the angle of the reference structure DPhPO-NH-DPhPO, with an angle of 180°. The difference between those structures is resulting from different hydrogen bond systems. Crystal structure analysis of DPhPO-NH-DPhPO confirmed a hydroxy phosphazene, as a polymeric chain with symmetric O···H···O hydrogen bonds resulting in an equidistant P-N bond length.

Behavior against hydrolysis. In organic and bioorganic chemistry, the products of the Staudinger reaction often undergo rapid hydrolysis delivering primary amines and phosphine (V) oxide. Staudinger products out of phosphor azides do not show the same lability.[38]

Thus the stability towards acidic hydrolysis of the synthesized product was tested in a simple NMR experiment exemplarily with two chosen compounds. DOPO-NH-DOPO and DPP-NH-DOPO were dissolved in acetonitrile/chloroform and treated with either water or 0.2 M hydrochloric acid, each at room temperature or 50°C for two hours. During the treatment, no change in the 31P-NMR signals could be observed. These results are consistent with previous studies conducted with N-phosphorylated iminophosphoranes as other Staudinger reaction products which are also stable against hydrolysis.[18,38] The corresponding spectra are shown below.

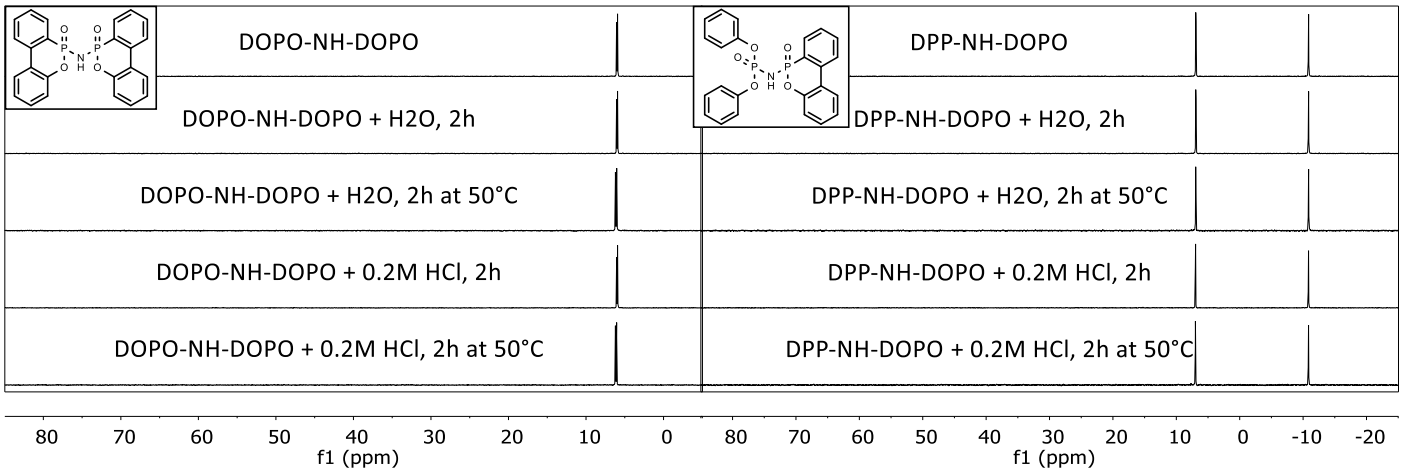

Figure 6. 31P {1H}-NMR spectra of DOPO-NH-DOPO and DPP-NH-DOPO during hydrolysis experiments recorded in a mixture of chloroform-d3 and Acetonitrile.

Thermal properties. To discuss and evaluate the possible application as flame retardant into either resin or thermoplastic polymer, the flame retardant must not decompose at temperatures below the resin´s curing or compounding temperature. The thermal decomposition of the bisphosphorylimides was investigated using thermogravimetric analysis (TGA). The TGA curves of the novel flame retardants are displayed in Figure 7, compared to the known flame retardant phosphazene $[NP(OPh)_2]_x$.

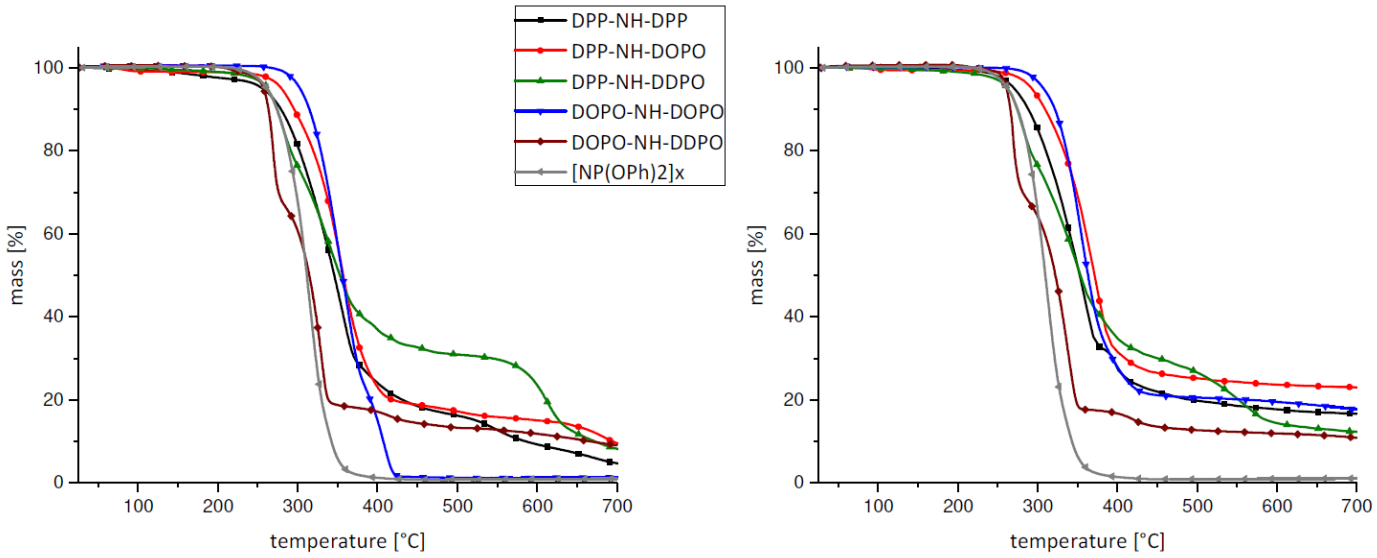

Figure 7. TGA curves of the new flame retardants under air (left) and nitrogen atmosphere (right).

DPP-NH-DPP is the least stable compound of this investigated array, starting to decompose before reaching 200°C under air and showing the biggest difference in decomposition temperature between air and nitrogen curves. In contrast, the curves of the other investigated compounds show less significant change. Based on hydrogen bridging and π-stacking stabilisation DOPO-NH-DOPO is the most stable of all investigated compounds, with a start of decomposition at 290°C (air) and 293°C (nitrogen). Also the thermal degradation of DOPO-NH-DOPO under air atmosphere is behaving similar to the reference substance $[NP(OPh)_2]_x$ while

showing degradation at higher temperature. Both substances are showing little residue and therefore enter the gas phase almost exclusivly. In Table 2 decomposition temperatures at 2% weight loss (T_{98}) as well as the temperatures corresponding to the maximum weight loss rate (T_{max}) and the residue at 700°C are listed.

Table 2. Thermal decomposition data of the additives based on TGA analysis recorded under nitrogen atmosphere and air

Compounds	Air atmosphere			Nitrogen atmosphere		
	T_{98} [°C]	T_{max} [°C]	$Residue_{700°C}$ [wt%]	T_{98} [°C]	T_{max} [°C]	$Residue_{700°C}$ [wt%]
DPP-NH-DPP	181.7	354.0	4.8	252.7	354.0	16.6
DPP-NH-DDPO	236.5	275.7	8.3	236.5	275.7	12.3
DPP-NH-DOPO	260.0	354.0	9.6	275.7	369.7	23.0
DOPO-NH-DOPO	290.4	353.4	1.4	292.3	354.5	17.7
DOPO-NH-DDPO	244.6	269.1	9.1	254.7	321.4	10.9
$[NP(OPh)_2]_x$	246.9	313.5	1.0	248.0	310.7	1.1

The results of DPP-NH-DDPO and DOPO-NH-DDPO display a two-step decomposition behavior with a more distinct second step in the curve of DPP-NH-DDPO. Both curves range around an initial decomposition temperature of 240°C. These results indicate a close relationship between the chemical environment of the phosphorus and the thermal stability of the molecule. DOPO-containing compounds include P-C moieties and have a higher thermal stability than their counterparts not containing P-C bonds. These results are consistent with the thermal degradation of triphenyl phosphate and triphenylphosphine oxide.[39]

TGA analyses in air atmosphere on compounds with phosphorus in different chemical environments result in more residue. The residue values of those compounds range from 8.3 to 9.6wt%, whereas the values for DPP-NH-DPP (4.8 wt%) and DOPO-NH-DOPO (1.4 wt%) as well as $[NP(OPh)_2]_x$ (1.0%) are significantly lower. Less residue indicate a ready transition into the gas phase, which is crucial for flame-retardants in order to perform an enhanced gas-phase activity.[40] Considering the residue values for air and nitrogen a significant rise in weight can be observed for almost all compounds. DOPO-NH-DDPO and $[NP(OPh)_2]_x$ are the only compounds showing only a minor increase of weight (1.0% and 0.1%) in nitrogen atmosphere.

Conclusions

Besides the previous researched Staudinger reaction as versatile tool in the synthesis of N-phosphorylated iminophosphoranes,[24,38] the possibility converting apparent pentavalent phosphorus compounds using the prototropic tautomeric equilibrium was confirmed. This reaction pathway opens up a new and convenient synthesis-pathway of bisphosphorylimides, leading to a tunable array of molecules with different phosphorus moieties. This opens up an easy access to tailored phosphoryl imides, useful as flame retardants or ligands.

Thus, five new bisphosphorylimides, with different chemical environments around the phosphorus, were synthesized using the Staudinger reaction. Moreover, the expected higher stability of the resulting products against hydrolysis was verified.

Single-crystal X-ray diffraction studies led to comparable results on molecular parameters and confirmed the bisphosphorylimides structure, rather than the iminophosphorane structure for the obtained products. In addition, the characteristic π-stacking of aromatic ring systems could be observed using the received parameters.

A relationship between the chemical environment around the phosphorus atom and the thermal stability of the corresponding compound was confirmed by TGA measurements. bisphosphorylimides with P-C moieties are thermally more stable than those with P-O moieties.

Experimental Section

General. Unless stated otherwise, solvents and chemicals were obtained from Fisher scientific and used as received without further purification. DOPO was supplied by Metadynea Austria GmbH.

Diffraction data of a suitable crystal were collected on a STOE STADIVARI diffractometer. The crystal was kept at 180 K during data collection. Using Olex2,[41] the structure was solved with the ShelXT[42] structure solution program using Intrinsic Phasing and refined with the ShelXL[43] refinement package using Least Squares minimisation. Visualizations of crystal structures were created with Mercury 3.10 from Cambridge Crystallographic Data Centre (CCDC).[44]

The thermogravimetric analysis (TGA) of the flame retardant additives was performed with a METTLER TOLEDO TGA 1 STAR System in a nitrogen or air environment, keeping a gas flow of 30 mL min^{-1}. The samples were heated starting from 25°C until 700°C with a rate of 10°C min-1.

Nuclear magnetic resonance (NMR) data were obtained on a Bruker NanoBay 300 spectrometer. Chemical shifts are reported as δ values relative to the solvent peak in ppm. Trimethylsilane was used as a standard. For all ^{31}P-NMR spectra proton decoupled and for ^{1}H-NMR spectra phosphorus decoupled measurement was used.

FT-IR spectra were recorded with a Thermo Scientific™ Nicolet™ 8700 spectrometer (Diamond ATR cell). Evaluation of the spectra was carried out with Thermo Scientific™ OMNIC™ FTIR Software.

6-Azidodibenzo[*c,e*][1,2]oxaphosphinin-6-oxide (DOPO-N3). Synthesis is following the procedure according to literature.[38]

Triethylammonium bis(6-oxidodibenzo[*c,e*][1,2]oxaphosphinin-6-yl)amide. DOPO (107.58 g, 497.65 mmol) and triethylamine (50.36 g, 497.65 mmol) were dissolved under argon atmosphere in a three-necked round-bottom flask fitted with a condenser, KPG stirrer and septum in dry CH_3CN. Subsequently a solution of DOPO-azide (127.99 g, 497.65 mmol) in CH_3CN was added dropwise at 70 °C and stirred until no more N_2 evolved. The reaction mixture was concentrated and the product was filtered and washed with dioxane to yield the colorless solid product.

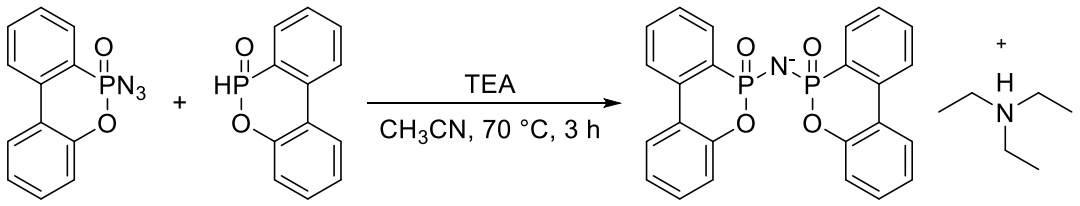

Yield: 71%. ^{31}P-NMR: (161.98 MHz, DMSO-d_6) δ 2.19 (s), 1.76 (s) ppm. ^{1}H-NMR: (400 MHz, DMSO-d_6) δ 9.76 (s, 1H), 7.97 (dt, *J*.7.9, 2.1 Hz, 1H), 7.93 (dt, *J* 8.3, 2.5 Hz, 1H), 7.73 (dqd, *J* 25.3, 7.3, 1.4 Hz, 1H), 7.53 (t, *J* 7.3 Hz, 1H), 7.34 (dt, *J* 22.5, 7.5 Hz, 3H), 7.16 (tt, J 7.5, 1.3 Hz, 1H), 7.04 (ddd, *J* 7.8, 6.1, 1.3 Hz, 1H), 2.88 (q, *J* 7.3 Hz, 6H), 1.01 (t, *J* 7.3 Hz, 9H) ppm. ^{13}C-NMR: (101 MHz, DMSO-d_6) 151.24 (t, *J* 3.0 Hz, 2C), 134.53 (t, *J* 3.1 Hz, 2C), 132.41 (dt, *J* 174.1, 3.1 Hz, 2C), 130.21 (s, 2C), 129.33 (d, *J* 2.1 Hz, 2C), 128.57 (t, *J* 4.8 Hz, 1C), 128.40 (t, *J* 4.6 Hz, 1C), 127.23 (td, *J* 7.2, 3.5 Hz, 2C), 125.03 (d, *J* 2.2 Hz, 2C), 123.76 (q, *J* 5.9 Hz, 2C), 123.40 (td, *J* 5.2, 2.6 Hz, 2C), 122.87 (s, 2C), 120.02 (q, *J* 2.5 Hz, 2C), 45.28 (s, 3C), 8.30 (s, 3C) ppm. MS calc. for $[C_{24}H_{17}NO_4P_2+H]^+$ 446.0706, found 446.0704.

6,6'-azanediylbis(dibenzo[*c,e*][1,2]oxaphosphinine 6-oxide) (DOPO-NH-DOPO). Triethylammonium bis(6-oxidodibenzo [c,e][1,2]oxaphosphinin-6-yl)amide (178.40 g, 326 mmol) was solved in chloroform and washed three times with 0.1 N aqueous hydrochloric acid and subsequently washed another three times with H_2O. The organic solution was concentrated in vacuo and the colorless product was filtered and washed with H_2O before it was dried at 120 °C. Crystals were obtained after recrystallization from isopropanol.

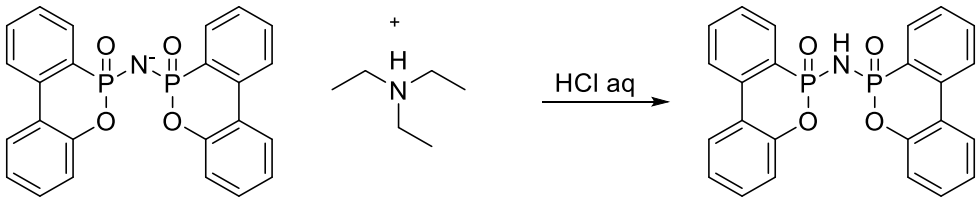

Yield: 99%. ^{31}P-NMR: (121.60 MHz, $CDCl_3$) δ 5.90, 5.70 ppm. ^{1}H-NMR: (300.38 MHz, $CDCl_3$) δ 8.32 (s, 1H), 8.18 - 8.05 (m, 4H), 7.90 - 7.67 (m, 4H), 7.62 - 7.50 (m, 2H), 7.44 - 7.37 (m, 2H), 7.29 -7.24 (m, 2H), 7.17 (dd, J 8.1, 1.2 Hz, 1H), 7.10 (dd, *J* 8.1, 1.2 Hz, 1H) ppm. ^{13}C-NMR: (75.53 MHz, $CDCl_3$) δ 148.93 (d, *J* 7.3 Hz, 1C), 148.84 (d, *J* 7.9 Hz, 1C), 135.07 (d, *J* 7.3 Hz, 2C), 133.24 - 132.82 (m, 2C), 130.41 (d, *J* 2.9 Hz, 2C), 129.88 (d, *J* 9.9 Hz, 1C), 129.71 (d, *J* 9.6 Hz, 1C), 128.38 (d, *J* 14.8 Hz, 2C), 125.33 (d, *J* 3.0 Hz, 2C), 124.92 (d, *J* 164 Hz, 1C), 124.69 (d, *J* 160.0 Hz, 1C), 124.53 (d, *J* 3.8 Hz, 2C), 123.81 (d, *J* 7.8 Hz, 1C), 123.75 (d, *J* 11.6 Hz, 1C), 121.45 (d, *J* 11.8 Hz, 1C), 121.32 (d, *J* 11.9 Hz, 1C), 119.87 (d, *J* 6.9 Hz, 2C) ppm. IR: (ATR): $\tilde{\nu}$ = 3050 (w, C_{aryl}-H), 2947 (w, N-H), 2700 (w, H-bridge), 1609 (w, C_{aryl}=C_{aryl}), 1597 (w, C_{aryl}=C_{aryl}) 1585 (w, C_{aryl}=C_{aryl}), 1561 (w, C_{aryl}=C_{aryl}), 1478 (m, N-H), 1448 (m, P-C_{aryl}), 1431 (m, P=N), 1352 (m), 1257 (s, P=O), 1207 (s), 1149 (s, P=O), 1121 (m, P-NH), 950 (vs, C_{aryl}-P-O), 781 (vs, C_{aryl}-H), 750 (vs, C_{aryl}-H) cm^{-1}. MS calc. for $[C_{24}H_{17}NO_4P_2+H]^+$ 446.0706, found $[M+H]^+$ 446.0709. TGA : T_{98} = 290.4°C (air) / 292.3°C (N_2). Smp.: 232.0°C

5,5-Dimethyl-1,3,2-dioxaphosphinane 2-oxide (DDPO)

Synthesis is following the procedure according to literature.[45]

6-((5,5-dimethyl-2-oxido-1,3,2-dioxaphosphinan-2-yl)amino)dibenzo[*c,e*][1,2]oxaphosphinine 6-oxide (DOPO-NH-DDPO). In a three-necked round-bottom flask fitted with a condenser, KPG stirrer and septum

DDPO (10.29 g, 40 mmol) and triethylamine (4.05 g, 40 mmol) were dissolved under argon atmosphere in dry CH_3CN. Subsequently, a solution of DOPO-azide (10.29 g, 40 mmol) in dry CH_3CN was added dropwise at 80 °C and refluxed. After no more N_2 evolved, the solvent was removed and the crude product was solved in chloroform to be treated with 0.1 M aqueous hydrochloric acid. Then, the organic layer was washed with H_2O three times before the solvent was removed.

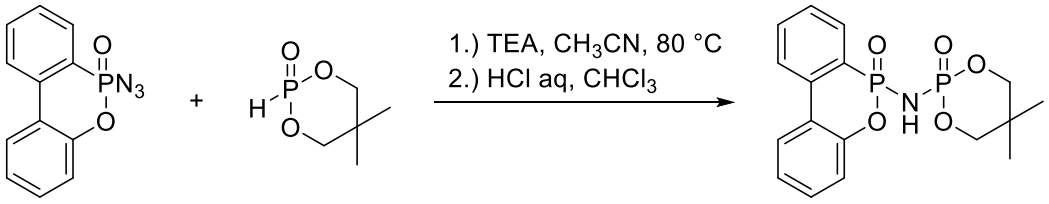

Yield: 56%. ^{31}P-NMR: (161.97 MHz, DMSO-d_6) δ 7.35 (d, *J* 4.9 Hz), -7.96 (d, *J* 5.0 Hz) ppm. ^{1}H-NMR: (400.13 MHz, DMSO-d_6) δ 8.29 - 8.17 (m, 2H), 7.93 (dd, *J* 14.9, 7.6 Hz, 1H), 7.79 (t, *J* 7.7 Hz, 1H), 7.63 (td, *J* 7.4, 3.1 Hz, 1H), 7.47 (t, *J* 7.7 Hz, 1H), 7.39 – 7.26 (m, 2H), 4.21 – 4.13 (m, 2H), 3.99-3.90 (m, 2H), 1.05 (s, 3H), 0.89 (s, 3H) ppm. ^{13}C-NMR: (100.63 MHz, DMSO-d_6) δ 149.00 (d, *J* 7.3 Hz, 1C), 135.21 (d, *J* 7.0 Hz, 1C), 133.20 (1C), 130.62 (1C), 129.76 (d, *J* 9.9 Hz, 1C), 128.58 (d, *J* 14.9 Hz, 1C), 125.55 (1C), 125.16 (d, *J* 164.0 Hz, 1C), 124.72 (1C), 123.99 (d, *J* 11.3 Hz, 1C), 121.65 (d, *J* 12.0 Hz, 1C), 120.13 (d, *J* 6.7 Hz, 1C), 76.71 (d, *J* 4.5 Hz, 1C), 31.67 (d, *J* 6.1 Hz, 1C), 25.54 (1C), 21.06 (1C), 20.04 (1C) ppm. IR (ATR): $\tilde{\nu}$ = 3050 (w), 1609 (w), 1597 (w), 1585 (w), 1561 (w), 1478 (m), 1448 (m), 1431 (m), 1352 (m), 1257 (s), 1243 (s), 1225 (s), 1207 (s), 1149 (m), 1121 (m), 1085 (w), 1044 (w), 967 (s), 950 (vs), 928 (s), 827 (m), 781 (s), 750 (vs), 712 (s) cm^{-1}. MS calc. for $[C_{17}H_{19}NO_5P_2\text{-}H]^-$ 378.0666, found 378.0665 $[M+H]^+$. TGA: T_{98} = 244.6°C (air) / 254.7°C (N_2). Smp.: 248.6°C.

***N*-(6-Oxidodibenzo[*c,e*][1,2]oxaphosphinin-6-yl)-*P,P*-diphenylphosphinic amide (DOPO-NH-DPhPO).** In a three-necked round-bottom flask fitted with a condenser, KPG stirrer and septum. Diphenylphosphine oxide (DPhPO) (10.29 g, 40 mmol) and triethylamine (4.05 g, 40 mmol) were dissolved under argon atmosphere in dry CH_3CN. Subsequently, a solution of DOPO-azide (10.29 g, 40 mmol) in dry CH_3CN was added dropwise at 80 °C and refluxed. After no more N_2 evolved, the solvent was removed and the crude product was solved in chloroform to be treated with 0.1 M aqueous hydrochloric acid. Then, the organic layer was washed with H_2O three times before the solvent was removed.

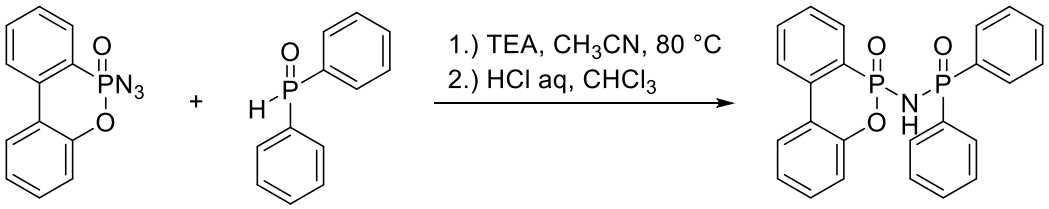

Yield: <5%

Because of the low yield further analytics could not be realized. Only some crystals could be obtained from the reaction mixture.

Tetraphenyl iminodiphosphate (DPP-NH-DPP). In a three-necked round-bottom flask fitted with a condenser and septum DPPA (5 g, 18.17 mmol) and DPPH (4.25 g, 18.17 mmol) were dissolved under nitrogen atmosphere in dry CH_3CN. Subsequently, triethylamin (1.84 g, 18.17 mmol) was added dropwise at 80 °C and

refluxed. After no more N_2 evolved, the solvent was removed and the crude product was solved in 75 mL chloroform to be treated with 150 mL 0.1 M aqueous hydrochloric acid. Then, the organic layer was washed five times with H_2O before the solvent was removed. The pure colorless product was recrystallized as colorless solid from chloroform/n-hexan.

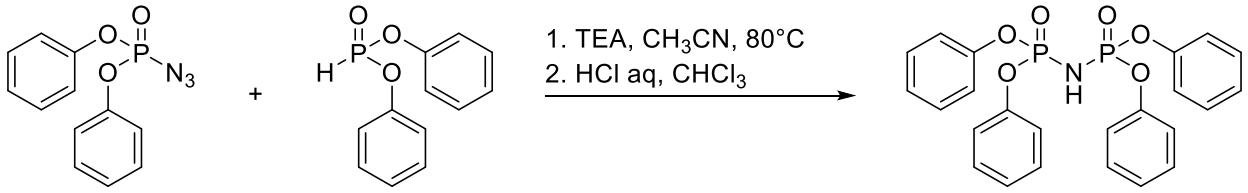

Yield: 82%. ^{31}P-NMR: (121.60, CDCl3): δ -10.85 (s) ppm. ^{1}H-NMR: (300.38 MHz, CDCl3): δ 7,3-7,1 (m, 20 H) ppm. ^{13}C-NMR: (75.54MHz, $CDCl_3$): δ 150.30 (t, J 3.6 Hz, 4C), 129.65 (s, 8C), 125.33 (s, 4C), 120.54 (t, J 2.4 Hz, 8C) ppm. IR (ATR): 3059 (w, C_{aryl}-H), 2966 (w, C_{aryl}-H), 2760 (w, H-bridge), 1588 (w, C_{aryl}=C_{aryl}), 1483 (m, N-H), 1404 (m, P-C_{aryl}), 1296 (m, P=O), 1242 (m, P=O), 1185 (s, P-N-H), 1155 (s, P-N-H), 1007 (m), 961 (m), 946, 911, 840, 774, 753, 689 (s, C_{aryl}-H) cm^{-1}. MS calc. for [$C_{24}H_{21}NO_6P_2$-H] 482.09, found 482.09 $[M+H]^+$
TGA: T_{98} = 181.7°C (air) / 252.7°C (N_2). Smp.: 94.1°C.

Diphenyl (6-oxidodibenzo[c,e][1,2]oxaphosphinin-6-yl)phosphoramidate (DPP-NH-DOPO). In a three-necked round-bottom flask fitted with a condenser and septum DPPA (6.39 g, 23 mmol) and DOPO (5.02 g, 23 mmol) were dissolved under nitrogen atmosphere in dry CH_3CN. Then triethylamine (2.35 g, 23 mmol) was added dropwise at 70 °C and the mixture was stirred until no more N_2 evolved. Then, the solvent was removed and the crude product was obtained. It was solved in 75 mL chloroform to be treated with 150 mL 0.2 M aqueous hydrochloric acid. The organic layer then was washed five times with H_2O before the solvent was removed. The pure colorless product was recrystallized from isopropanol.

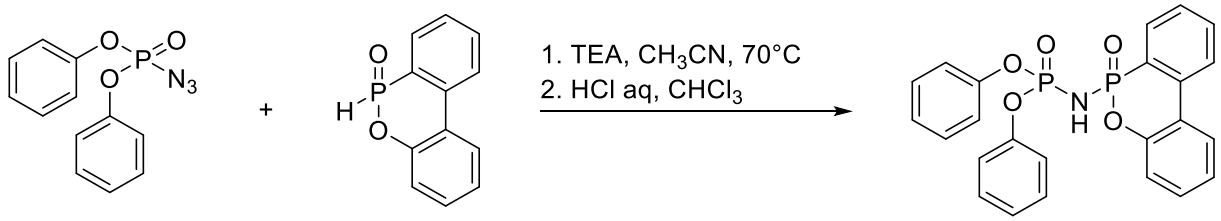

Yield: 95%. ^{31}P-NMR: (121.60, CDCl3) δ 2.87 ppm (d, J 44.2 Hz), -10.39 ppm (d, J 44.2 Hz). ^{1}H-NMR: (300.38 MHz, CDCl3) δ 7.99-7,91 (m, 2H), 7.69-7.63 (m, 2H), 7.35-7.11 (m, 12H), 7.45 (m, 1H) ppm. ^{13}C-NMR: (75.54 MHz, $CDCl_3$): δ 150.23 (d, J 3.8 Hz, 1C), 150.14 (d, J 3.9Hz, 1C), 149.61 (d, *J* 7.5 Hz, 1C), 136.41 (d, *J* 7.7 Hz, 1C), 133.13 (d, *J* 2.5 Hz, 1C), 130.23 (d, *J* 4.1 Hz, 1C), 129.62-129.55 (m, 4C), 128.11 (d, *J* 15.4 Hz, 1C), 125.30-125.21 (m, 2C), 124.84-124.75 (m, 1C), 124.46 (d, J 4.9 Hz, 1C), 123.27 (d, *J* 12.2 Hz, 1C), 121.42 (d, *J* 12.1 Hz, 1C), 120.71 (d, J 4.8 Hz, 2C), 120.57 (d, *J* 4.9 Hz, 2C), 120.17 (d, *J* 7.4 Hz, 1C) ppm. IR (ATR): $\tilde{\nu}$ = 3058 (w, C_{aryl}-H), 2896 (w, C_{aryl}-H), 2715 (w, H-bridge), 2636 (w), 1595 (w, C_{aryl}=C_{aryl}), 1482 (m, N-H), 1450 (m, P-C_{aryl}), 1383 (m), 1274 (m, P=O), 1215 (m, P=O), 1186 (s, P-N-H), 1161 (s, P-N-H), 1120 (m, C_{aryl}-O), 1006 (m, P-O-C), 961 (vs, C_{aryl}-P-O), 937, 924 (s, C_{aryl}-H), 897, 845, 791 (w, C_{aryl}-H), 751 (vs, C_{aryl}-H), 692 (m, C_{aryl}-H) cm^{-1}.
MS calc. for [$C_{24}H_{19}O_5P_2N_1$-H] 464.08, found 464.08 $[M+H]^+$. TGA: T_{98} = 260.0°C (air) / 275.7°C (N_2). Smp.: 178.0°C.

Diphenyl (5,5-dimethyl-2-oxido-1,3,2-dioxaphosphinan-2-yl)phosphoramidate (DPP-NH-DDPO). In a three-necked round-bottom flask fitted with a condenser and septum DPPA (5 g, 18 mmol) and DDPO (2.73 g, 18 mmol) were dissolved under nitrogen atmosphere in dry CH_3CN. Then triethylamin (1.83 g, 18 mmol) was added dropwise at 80 °C and the mixture was stirred until no more N_2 evolved. Then, the solvent was removed and the crude product was obtained. The crude product was solved in 75 mL chloroform to be treated with 150 mL 0.2 M aqueous hydrochloric acid for 5h. The organic layer was washed five times with H_2O before the solvent was removed. The pure product was obtained after crystallization from the received oil.

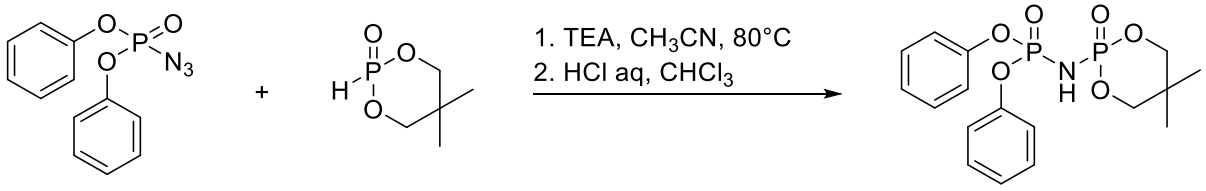

Yield: 21%. ^{31}P-NMR: (121.60, CDCl3) δ -8.28 (d, 1 P, *J* 8.5 Hz), -8.62 (d, 1 P, *J* 8.4 Hz) ppm. ^{1}H-NMR: (300.38 MHz, CDCl3) δ 7.13-7.35 (m, 10H), 4.26 (d, *J* 10.8 Hz, 2H), 3.87 (d, *J* 10.9 Hz, 2H), 1.16 (s, 3H), 0.89 (s, 3H) ppm. ^{13}C-NMR: (75.54 MHz, $CDCl_3$) δ 150.31 (t, *J* 3.6 Hz, 2C), 129.64 (s, 4C), 125.40 (s, 2C), 120.78 (t, J 2.4 Hz, 4C), 77.71 (d, *J* 6.5 Hz, 2C), 31.98 (d, *J* 6.9 Hz, 1C), 21.89 (s, 1C), 20.50 (s, 1C) ppm. IR (ATR): $\tilde{\nu}$ = 2985 (w, C_{aryl}-H), 2956 (w, C_{alkyl}-H), 2703 (w, H-bridge), 1589 (w, C_{aryl}=C_{aryl}), 1485 (m, N-H), 1370 (w, C_{alkyl}-H), 1283 (m, C_{alkyl}-C_{alkyl}), 1263 (m, C_{alkyl}-C_{alkyl}), 1243 (m, P=O), 1208 (m, P=O), 1183 (s, P-N-H), 1157 (s, P-N-H), 1067 (m, P-O-C), 1008 (s, P-O-C), 969, 935, 864, 839, 773, 690 (s, C_{aryl}-H) cm^{-1}. MS calc. for [$C_{17}H_{21}O_6P_2N_1$-H] 398.09, found 398.09 [M+H]$^+$ TGA: T_{98} = 236.5°C / 236.5°C (N_2). Smp.: 131.9°C.

Supplementary Material

Crystallographic data of DPP-NH-DPP, DPP-NH-DOPO, DOPO-NH-DOPO and DOPO-NH-DPhPO are shown in the supplementary information.

References

1. He, X.; Ji, Y.; Jin, Y.; Kan, S.; Xia, H.; Chen, J.; Liang, B.; Wu, H.; Guo, K.; Li, Z. *J. Polym. Sci. Part A: Polym. Chem.*, **2014**, *52*, 1009–1019. https://doi.org/10.1002/pola.27082
2. Lu, G.-Z.; Han, H.-B.; Li, Y.; Zheng, Y.-X. *Dyes and Pigments* **2017**, *143*, 33–41, https://doi.org/10.1016/j.dyepig.2017.04.016
3. Zhou, Y.-H.; Xu, J.; Wu, Z.-G.; Zheng, Y.-X. *Journal of Organometallic Chemistry* **2017**, *848*, 226–231, https://doi.org/10.1016/j.jorganchem.2017.07.039
4. Liu, N.; Wang, Y.; He, C.,*Journal of Radioanalytical and Nuclear Chemistry* **2016**, *308*, 393–401, https://doi.org/10.1007/s10967-015-4454-1
5. Tsoupras, A.B.; Roulia, M.; Ferentinos, E.; Stamatopoulos, I.; Demopoulos, C.A.; Kyritsis, P. *Bioinorganic chemistry and applications*. https://doi.org/2010, 10.1155/2010/731202.

6. Wang, G.-C.; Sung, H.H.Y.; Dai, F.-R.; Chiu, W.-H.; Wong, W.-Y.; Williams, I.D.; Leung, W.-H., *Inorganic chemistry* **2013**, *52*, 2556–2563 https://doi.org/10.1021/ic302567e
7. Sun, Z.; Hou, Y.; Hu, Y.; Hu, W., *Materials Chemistry and Physics*, **2018**, *214*, 154–164. https://doi.org/10.1016/j.matchemphys.2018.04.065
8. Yang, S.; Hu, Y.; Zhang, Q., *High Performance Polymers*, **2019**, *31*, 186–196. https://doi.org/10.1177/0954008318756496
9. Li, Q.-L.; Huang, F.-Q.; Wei, Y.-J.; Wu, J.-Z.; Zhou, Z.; Liu, G. *Materials Science* **2018**, *24*, https://doi.org/10.5755/j01.ms.24.4.18606
10. Liu, X.; Liang, B., *Materials Research Express* **2017**, *4*, 125103. https://doi.org/10.1088/2053-1591/aa9dba
11. Kloock, C. Synthesis of Potential Phosphorus-Nitrogen Containing Flame Retardants. Honors Thesis, 2015.
12. Camino, G.; Luda, M.P.; Costa, L. *Le Journal de Physique IV*, **1993**, *03*, C7-1539-C7-1542. https://doi.org/10.1051/jp4:19937240
13. Factor, A. *Journal of Chemical Education*, **1974**, *51*, 453. https://doi.org/10.1021/ed051p453
14. Lu, S.-Y.; Hamerton, I. *Progress in Polymer Science* **2002**, *27*, 1661–1712. https://doi.org/10.1016/S0079-6700(02)00018-7
15. Rakotomalala, M.; Wagner, S.; Döring, M. *Materials (Basel, Switzerland)*, **2010**, *3*, 4300–4327. https://doi.org/10.3390/ma3084300
16. Wazarkar, K.; Kathalewar, M.; Sabnis, A. *Polymer-Plastics Technology and Engineering* **2016**, *55*, 71–91. https://doi.org/10.1080/03602559.2015.1038839
17. Staudinger, H.; Meyer, J. *Helvetica Chimica Acta*, **1919**, *2*, 635–646. https://doi.org/10.1002/hlca.19190020164
18. Baldwin, R.A.; Washburn, R.M. *J. Am. Chem. Soc.* **1961**, *83*, 4466–4467. https://doi.org/10.1021/ja01482a038
19. Gololobov, Y.G.; Zhmurova, I.N.; Kasukhin, L.F. *Tetrahedron* **1981**, *37*, 437–472. https://doi.org/10.1016/S004020(01)92417-2
20. Gololobov, Y.G.; Kasukhin, L.F. *Tetrahedron* **1992**, *48*, 1353–1406. https://doi.org/10.1016/S0040-4020(01)92229-X
21. Riesel, L.; Steinbach, J.; Herrmann, E. *Z. Anorg. Allg. Chem.* **1983**, *502*, 21–28. https://doi.org/10.1002/zaac.19835020704
22. Bräse, S.; Gil, C.; Knepper, K.; Zimmermann, V., *Angewandte Chemie (International)* **2005**, *44*, 5188–5240. https://doi.org/10.1002/anie.200400657
23. Köhn, M.; Breinbauer, R., *Angew. Chem.*, **2004**, *116*, 3168–3178. https://doi.org/10.1002/ange.200401744.
24. Micle, A.; Miklášova, N.; Varga, R.A.; Pascariu, A.; Pleşu, N.; Petric, M.; Ilia, G. *Tetrahedron Letters* **2009**, *50*, 5622–5624. https://doi.org/10.1016/j.tetlet.2009.07.112
25. Shi, E.; Pei, C., *Synthesis* **2005**, *2005*, 166. https://doi.org/10.1055/s-2004-837286
26. Low, J.E. Investigation of Silicon- and/or Nitrogen-containing Phosphorus-based Compounds as Flame Retardants for Cotton Textiles, 2017.
27. Nielsen, M.L., *Inorg. Chem.* **1964**, *3*, 1760–1767.

https://doi.org/10.1021/ic50022a024
28. Herrmann, E.; Nouaman, M.; Zak, Z.; Gromann, G.; Ohms, G. *Z. Anorg. Allg. Chem.* **1994**, *620*, 1879–1888, https://doi.org/10.1002/zaac.19946201108
29. Wilkening, I.; del Signore, G.; Hackenberger, C.P.R. *Chem. Comm.* **2011**, *47*, 349–351. https://doi.org/10.1039/C0CC02472D
30. Nöth, H., *Zeitschrift für Naturforschung B* **1982**, *37*, 1491–1498. https://doi.org/10.1515/znb-1982-1201
31. Janiak, C., *J. Chem. Soc., Dalton Trans.* **2000**, 3885–3896. https://doi.org/10.1039/B003010O
32. Sinnokrot, M.O.; Valeev, E.F.; Sherrill, C.D. *J. Am. Chem. Soc.* **2002**, *124*, 10887–10893 https://doi.org/10.1021/ja025896h
33. Wagner, S.; Rakotomalala, M.; Bykov, Y.; Walter, O.; Döring, M. *Heteroatom Chem.* **2012**, *23*, 216–222. https://doi.org/10.1002/hc.21006
34. Burk, B. Entwicklung neuer Flammschutzmittel basierend auf Derivaten des 9,10-Dihydro-10-oxaphosphaphenanthren-10-oxids; Verlag Dr. Hut: München, 2016.
35. Müller, P.; Bykov, Y.; Walter, O.; Döring, M. *Heteroatom Chem.* **2012**, *23*, 383–394, https://doi.org/10.1002/hc.21028
36. Kulpe, S.; Seidel, I.; Herrmann, E., *Cryst. Res. Technol.* **1984**, *19*, 661–668. https://doi.org/10.1002/crat.2170190517
37. Bolboaca, M.; Stey, T.; Murso, A.; Stalke, D.; Kiefer, W. *Applied spectroscopy* **2003**, *57*, 970–976. https://doi.org/10.1366/000370203322258931
38. Weinert, M.; Fuhr, O.; Döring, M. *Arkivoc* **2019**, 278–293. https://doi.org/10.24820/ark.5550190.p010.704
39. Horrocks, A.R.; Davies, P.J.; Kandola, B.K.; Alderson, A. *Journal of Fire Sciences* **2007**, *25*, 523–540. https://doi.org/10.1177/0734904107083553
40. Schartel, B., *Materials (Basel, Switzerland)* **2010**, *3*, 4710–4745. https://doi.org/10.3390/ma3104710
41. Dolomanov, O.V.; Bourhis, L.J.; Gildea, R.J.; Howard, J.A.K.; Puschmann, H. *J Appl Crystallogr.* **2009**, *42*, 339–341. https://doi.org/10.1107/S0021889808042726
42. Sheldrick, G.M. *Acta crystallographica. Section A, Foundations and advances* **2015**, *71*, 3–8. https://doi.org/10.1107/S2053273314026370
43. Sheldrick, G.M. *Acta crystallographica. Section C, Structural Chemistry* **2015**, *71*, 3–8. https://doi.org/10.1107/S2053229614024218
44. Macrae, C.F.; Edgington, P.R.; McCabe, P.; Pidcock, E.; Shields, G.P.; Taylor, R.; Towler, M.; van de Streek, J. *J Appl Crystallogr*. **2006**, *39*, 453–457. https://doi.org/10.1107/S002188980600731X
45. Oussadi, K.; Montembault, V.; Belbachir, M.; Fontaine, L., *J. Appl. Polym. Sci.* **2011**, *122*, 891–897. https://doi.org/10.1002/app.34193.